Improving model capability in simulating spatiotemporal variations and flow contributions of nitrate export in tile-drained catchments

Peiyu Cao[a], Chaoqun Lu[a], William Crumpton[a], Matthew Helmers[b], David Green[a], Greg Stenback[a]

[a] Department of Ecology, Evolution, and Organismal Biology, Iowa State University, 251 Bessey Hall, 2200 Osborn Dr., Ames, IA 50011, USA

[b] Department of Agricultural and Biosystems Engineering, Iowa State University, 4354 Elings, 605 Bissell Rd., Ames, IA 50011, USA

Abstract

It is essential to identify the dominant flow paths, hot spots and hot periods of hydrological nitrate-nitrogen (NO_3-N) losses for developing nitrogen loads reduction strategies in agricultural watersheds. Coupled biogeochemical transformations and hydrological connectivity regulate the spatiotemporal dynamics of water and NO_3-N export along surface and subsurface flows. However, modeling performance is usually limited by the oversimplification of natural and human-managed processes and insufficient representation of spatiotemporally varied hydrological and biogeochemical cycles in agricultural watersheds. In this study, we improved a spatially distributed process-based hydro-ecological model (DLEM-catchment) and applied the model to four tile-drained catchments with mixed agricultural management and diverse landscape in Iowa, Midwestern US. The quantitative statistics show that the improved model well reproduced the daily and monthly water discharge, NO_3-N concentration and loading measured from 2015 to 2019 in all four catchments. The model estimation shows that subsurface flow (tile flow + lateral flow) dominates the discharge (70%-75%) and NO_3-N loading (77%-82%) over the years. However, the contributions of tile drainage and lateral flow vary remarkably among catchments due to different tile-drained area percentages and the presence of farmed potholes (former depressional wetlands that have been drained for agricultural production). Furthermore, we found that agricultural management (e.g. tillage and fertilizer management) and catchment characteristics (e.g. soil properties, farmed potholes, and tile drainage) play important roles in predicting the spatial distributions of NO_3-N leaching and loading. The simulated results reveal that the model improvements in representing water retention capacity (snow processes, soil roughness, and farmed potholes) and tile drainage improved model performance in estimating discharge and NO_3-N export at a daily time step, while improvement of agricultural management mainly impacts NO_3-N export prediction. This study underlines the necessity of characterizing catchment properties, agricultural management practices, flow-specific NO_3-N movement, and spatial heterogeneity of NO_3-N fluxes for accurately simulating water quality dynamics and predicting the impacts of agricultural conservation nutrient reduction strategies.

1 Introduction

The modern agricultural system coupled with fertile soil conditions and a suitable climate environment has made the US Corn Belt one of the most productive agricultural regions in the world (Gonzalo et al., 2022). Substantial nitrogen (N) synthetic fertilizer and manure supplementation for crop production have also made this region a hotspot of N inputs in the US. (Bian et al., 2021; Cao et al., 2018). Total N inputs in this region often exceed crop utilization, resulting in a substantial N surplus (Lu et al., 2019; Zhang et al., 2021), which leads to a waste of resources and degrading water quality (Baron et al., 2013). The increased leaching of nitrate-nitrogen (NO_3-N) from agricultural areas in this region is identified as a primary contributor to hypoxia in the Gulf of Mexico (Jones et al., 2018). Therefore, it is essential to identify the dominant processes, critical areas, and time periods of NO_3-N losses for implementing effective agricultural conservation practices to mitigate the agriculture-derived water quality issues. Spatially distributed process-based modeling with adequate representation of the hydrological-biogeochemical cycles is a promising tool to quantify the NO_3-N leaching and transport processes and to predict the efficiency of multiple management practices in reducing NO_3-N loads in agricultural watersheds (Ren et al., 2022).

Simulating the dynamics of NO_3-N export at the watershed outlet is challenging as they reflect complicated impacts of climate variation, watershed characteristics, human management, and hydrological and biogeochemical cycles. Agricultural management plays a critical role in determining NO_3-N input sources in agricultural watersheds. For example, crop rotation and N fertilizer management (rate, timing, method, and form) significantly impact the magnitude and seasonality of N inputs (Cao et al., 2018). Constrained by local environmental conditions, the N biogeochemical transformation is generally complex and highly heterogeneous, which influences the dynamics of NO_3-N availability over space and time. Furthermore, the spatiotemporal hydrological processes connect the agriculture-derived NO_3-N sources and transport them to streams. Due to the divergence in hydrological connectivity and flow travel time, water and N fluxes that flow along separate pathways contribute differently to in-stream NO_3-N dynamics over time. This is particularly important in tile-drained watersheds in the Midwest. Tiles that are installed below the soil surface profoundly alter the water and nutrient balance of agricultural watersheds by shortening groundwater travel time and quickly removing excess water from the soil (Schilling et al., 2015). In the Prairie Pothole Region of North America, small depressional wetlands were formed by glacial activity and subsequent thawing. These depressions have been converted for agricultural practices such as crop cultivation and livestock grazing (defined as farmed pothole hereafter). Coupled with tile drains, farmed potholes significantly change hydrological and biogeochemical cycles in this region by intercepting runoff and retaining nutrients (Hayashi et al., 2016; Tomer et al., 2003). Therefore, insufficient representation of agricultural management, catchment characteristics (e.g. tile drainage and farmed potholes), and their interactions undermines model performance in tracking NO_3-N leaching and delivery along water flows.

A wide variety of modeling efforts have attempted to evaluate the impacts of various management practices on agricultural non-point source of NO_3-N losses at both field-level and large watershed-level in the US Corn Belt (Ren et al., 2022; Tahmasebi Nasab and Chu, 2020).

However, due to the scarcity of long-term monitoring data and spatially detailed farming practices information, very few modeling studies have focused on the scale at which the NO_3-N loads are delivered to surface water systems (defined as delivery-scale hereafter, Ikenberry et al., 2017). The delivery-scale catchment is the ideal spatial scale for identifying model performance and assessing the effectiveness of agricultural conservation practices since this scale reflects field-scale processes and field-to-stream transport but excludes in-stream NO_3-N removal effects. Most models that are widely used in this region are semi-distributed, for example, the Soil Water Assessment Tool (Wellen et al., 2015), in which the watershed is disaggregated into homogenous hydrological response units (HRU) based on topography, soil type, and land use. However, the spatial heterogeneity of environmental factors within HRU is averaged, which may lead to mismatches between natural units (e.g. landscape and slope) and agricultural management boundary (e.g. field) within the HRU (Du et al., 2005; Ren et al., 2022). Furthermore, the aggregated water management (e.g. subsurface drainage, making the system leakier) and landscape characteristics (e.g. farmed potholes that enhance water retention) within the HRU have mixed up the bi-directional water dynamics and overlooked the spatiotemporal dynamics of transport processes. Consequently, the biogeochemical transformation and transport processes of water and N fluxes regulated by climate, agricultural management, and catchment characteristics may be misrepresented in semi-distributed models due to such management-water-N decoupling.

The modeling tool we used in this study is derived from the spatially distributed, process-based Dynamic Land Ecosystem Model 2.0 (DLEM 2.0) that is designed to simulate the coupled water-N-carbon cycling within the plant-soil-water-river continuum from the grid to the regional level. This model has been extensively validated and applied to quantify water flow and N loading from the Mississippi river basin and its sub-basins (Liu et al., 2013; Lu et al., 2020; Zhang et al., 2022). Based upon DLEM 2.0, we developed a new DLEM version, named DLEM-catchment, which has better representations of management practices and unique features to mimic flow-specific water and N transport through farmed potholes and tile lines. Here, a catchment is defined as topographically-based and elevation-derived sub-areas of a watershed, excluding the impacts of upstream sources (Hill et al., 2017).

In this study, we applied DLEM-catchment to four tile-drained delivery-scale agricultural catchments in Iowa in the Midwestern US at a 30-m resolution. Using historical weather conditions, field-level practice information, and other input drivers to force the model, we confronted the modeled results with daily observations of water discharge and NO_3-N export from 2015 to 2019. The main objectives of this study were 1) to improve model representation of management, physical and biogeochemical processes in reproducing daily observations of discharge and NO_3-N exports from tile-drained catchments, 2) to assess the relative contributions of distinct hydrologic transport pathways to dynamics of discharge and NO_3-N exports, 3) to evaluate how agricultural management and catchment characteristics translate to the spatial pattern of NO_3-N concentration and loading fluxes, and 4) to quantify the contribution of key model improvements to the estimation of water and N loading dynamics.

2 Methods and Procedures

2.1 Study Area

Four catchments in Iowa were simulated for this study (Fig. 1): the RS and KS catchments located in Story County, and the LP and WW catchments located in Floyd County. These catchments are in a temperate region characterized by a humid continental climate, with an average annual precipitation of 1100 mm. The temperature throughout the year ranges widely from -32 ºC to 38 ºC with an average annual temperature of 9 ºC. The snow season typically spans from late November to early April. All four catchments drain into first-order streams with drainage areas ranging from 2.1 to 4.6 km^2. The RS and KS catchments are located in the Des Moines Lobe of Iowa (DML-IA), a geomorphic region of the state that contains a large number of farmed potholes, and as such each catchment features multiple, drained depressional wetlands. In contrast, the LP and WW catchments are situated outside of the DML-IA, and do not include drained depressional wetlands. Land use was similar in the four catchments with more than 80% of the area of each watershed used for corn-soybean (CS) and continuous corn (CC) cropping systems. These catchments are well representative of tile-drained watersheds that do and do not host farmed potholes, and feature variability in climate, catchment characteristics, and agricultural management, which makes them especially suitable to develop and evaluate model predictions regarding water discharge and nitrate export (Table 1).

2.2 Hydrology and NO_3-N concentration measurements

The daily discharge and NO_3-N concentrations for 2015 through 2019 were measured and processed from sub-daily observations taken close to the outlet of each catchment. Full details related to the discharge and NO_3-N measurements can be found in Crumpton et al. (2020). To quantify the contribution of different flow pathways to total catchment discharge, we separated the measured daily discharge into surface runoff and subsurface flow components (tile flow + lateral flow) using four hydrograph separation approaches, including the local minimum method (LMM), the one parameter digital filter (OPD), the recursive digital filter (RDF), and the end member mixing model (EMM). The LMM connects the lowest points on the hydrograph with straight lines to estimate surface runoff and subsurface flow (Sloto and Crouse, 1996). The digital methods, OPD (Lyne and Hollick, 1979) and RDF (Eckhardt, 2005), were used to separate high frequency waves (surface runoff) and low frequency waves (subsurface flow). We applied a filter parameter of 0.98 and a BFI maximum of 0.8 to RDF (Schilling and Jones, 2019). EMM is a tracer-based method that separates hydrograph into two or more components by linearly mixing conservative tracers. In this study, we applied EMM by combining measurements of stream discharge and NO_3-N concentration (Ikenberry et al., 2017).

2.3 DLEM Improvements

Despite its success in simulating various hydrological and biogeochemical cycling processes at the large watershed and regional scales, DLEM 2.0 required modifications to reproduce discharge and N loading in catchments of smaller size due to the over-simplified processes, less data availability, and difficulty in calibration and validation. To meet this need, in this study, we improved DLEM 2.0 (DLEM-catchment) by adding a two-layer snow model, soil roughness, and farmed potholes fill and spill dynamics to increase water retention capacity. In addition, we improved flow generation and transport by enhancing subsurface flow separation, flow travel time, and flow routing (Fig. 2). Moreover, we integrated various agricultural management practices into the model based on field records (see supplementary material for detailed model improvement).

2.4 Data Preparation

In order to characterize the environmental changes and prepare model input drivers, we collected and processed a number of time-variant and invariant databases from multiple sources into model-compatible formats. All gridded geospatial data was resampled to 30-m resolution grids, and time-series input drivers were compiled to drive the model run over the period 2000 to 2019. The detailed information is listed in Table S2.

Climate: Daily solar radiation and temperature (maximum and minimum) were obtained from the three closest climate sites, IAC005 (RS), IA0200 (KS), and IA1402 (LP and WW), through the Iowa Environmental Mesonet (IEM, 2021). Daily mean temperatures were calculated by averaging the daily maximum and minimum temperatures. Daily precipitation was extracted from the IEM geospatial rainfall data product from a particular point within each catchment. Given their small areas, we assumed each catchment experienced temporally varying, but spatially uniform atmospheric conditions.

Atmospheric components: Monthly CO_2 concentration was retrieved from the dataset developed by Wei et al. (2014). Annual geospatial ammonium and nitrate maps were obtained from the National Atmospheric Deposition Program (NADP, https://nadp.slh.wisc.edu/maps-data/ntn-gradient-maps/).

Geographic characteristics: The 10-m resolution USGS National Elevation Dataset (https://apps.nationalmap.gov/downloader/) was used to calculate topographic indexes and delineate hydrological parameters. The distribution and properties (maximum area and depth) of farmed potholes were obtained from McDeid et al. (2019). Soil properties were obtained from the gridded Soil Survey Geographic Database (gSSURGO, https://datagateway.nrcs.usda.gov/GDGHome_DirectDownLoad.aspx). Grids of likely tile-drained areas for each catchment were derived by intersecting gSSURGO soils identified as "somewhat poorly drained", "poorly drained", or "very poorly drained" with elevation grid cells having local slopes of less than 8% (Valayamkunnath et al., 2020).

Land use and land cover: Annual land use data, including crop type and distributions, from 2000 to 2019 at a 30-m resolution were obtained from the National Agricultural Statistics Service Crop Data Layer (CDL, https://nassgeodata.gmu.edu/CropScape/).

Agricultural management: Field-level farm management information was retrieved from the field records of partnering farmers, including tillage type and timing, cover crop management, and synthetic N fertilizer and manure management information such as application rates, timing, and form (Fig. S2).

2.5 Model calibration and simulation

DLEM 2.0 has been rigorously calibrated and validated against the measurements of the carbon cycle, the N cycle, and water flow at site-specific, regional, and global scales (Lu et al., 2022, 2020; Tian et al., 2010; Yu et al., 2018). We further calibrated the key parameters related to plant growth using the county average corn and soybean yield from 2000 to 2019, which is essential for simulating water balances (e.g. transpiration) and N balances (e.g. N uptake and plant residual N). In this work, the snowpack depth obtained from nearby weather stations was used to calibrate the parameters that determine the snowfall-rainfall ratio (Fig. S3). We also calibrated the key parameters controlling hydrological and biogeochemical processes and validated the simulated discharge and NO_3-N export against the measurements in the four study catchments from 2015 to 2019. The description of the key model parameters is detailed in Table S2. The model was first run to get the 2000 baseline of C, N, and water pools by repeatedly using land use data for 2000, and the 20-year, 1980-1999, mean climate. The model was then run to simulate the daily discharge and in-stream NO_3-N concentration using driving data from 2000 to 2019.

2.6 Model performance evaluation

We adopted three widely used indices to evaluate model performance: the Nash-Sutcliffe Efficiency (NSE) (Nash and Sutcliffe, 1970), the Percent Bias (PBIAS), and the Kling-Gupta Efficiency (KGE) (Gupta et al., 2009)). The NSE value measures how well the simulated values agree with measured values. NSE values range from $-\infty$ to 1, with the value of 1 considered a perfect match. The PBIAS measures the average tendency of the simulated values to be larger or smaller than their corresponding observations, with an optimal value of zero. The KGE value, ranging from $-\infty$ to 1, measures the composite performance that considers association, similarity in variability, as well as distance between observation and simulation. The closer to 1, the more accurate the model is.

We judged the model performance for NSE and PBIAS based on the evaluation criteria by Moriasi et al. (2015) and KGE by Tahmasebi Nasab and Chu (2020) (Table S3). Due to general poor model performance in simulating in-stream NO_3-N concentration among studies, Moriasi et al. (2015) suggested criteria of NSE and PBIAS only for monthly NO_3-N loading. Given no consensus on prediction accuracy of NO_3-N concentration that is very dynamic, here, we applied these criteria for evaluating daily and monthly NO_3-N concentration simulations, which may underrate our model performance. In addition to these statistical measures, the reliability of model outputs was judged through the graphical presentations of the predicted and observed data.

3 Results

3.1 Discharge and In-stream Nitrate Concentration

Given the limited length of water quality monitoring data, we calibrated the key parameter values by using annual ranges of observations, and further evaluated the model performance in simulating discharge, NO_3-N concentration and loading against daily and monthly observations from 2015 to 2019 in four catchments. The predicted daily discharge over the study period is satisfactory for all the four catchments according to the NSE metric, whereas PBIAS and KGE values indicate good model simulations (Table 2). All three criteria indices for monthly discharge indicate good to very good model performance at four catchments. The simulated daily discharge reasonably captures the rise and fall of the observed hydrographs. However, some discrepancies in stream peaks and low flows are apparent (Fig. 3). For example, the model underestimates peak flows for some storm events in the KS and WW catchments, especially for simulations of wet years.

As shown in Table 2, the statistic indices for modeling the daily in-stream NO_3-N concentrations from four catchments are within the satisfactory range with respect to KGE > 0.5, and of very good range with respect to PBIAS (< 15%). Because we adopt the classification standard for nitrate loading that is likely too strict for assessing the prediction accuracy of NO_3-N concentration, it is not surprising the model performance in estimating daily NO_3-N concentration from two catchments (RS and LP) is ranked unsatisfactory using NSE (i.e. NSE < 0.35, Table 2). The simulated daily NO_3-N concentration generally matches observations, with good presentation of intra-annual and seasonal dynamics (Fig. 4). Some discrepancies are found for the lows in fall and winter months, and for peak flows in early spring periods. For example, the model underestimates NO_3-N concentration during the fall and winter of 2014/2015 in the RS and KS catchments, and overestimates that in the early spring of 2018 in the RS catchment. In addition, simulated daily NO_3-N concentration shows more short-term fluctuations than observations. In contrast, the simulated monthly NO_3-N concentration is ranked acceptable to good by all indices. Both daily and monthly simulations of NO_3-N loading fall within good range, except for daily loading in the KS catchment, which is lower than the satisfactory limit. The simulated daily NO_3-N loading adequately captures the peaks and lows of observations, except that some peak loads were underestimated (Fig. S4). NO_3-N loading is the product of discharge and NO_3-N concentration. Given the good performance in discharge simulation, the uncertainty in predicting NO_3-N loading may be mainly attributed to simulated NO_3-N concentrations.

3.2 Contributions of Flows to Discharge and Nitrate Loading

In this study, we quantified the contributions of daily surface runoff, tile drainage, and lateral flows to water discharge at the catchment outlet. The simulated subsurface flow (tile flow + lateral flow) is the major contributor to discharge in four catchments, with annual base flow indices (BFI, that is the ratio of subsurface flow to discharge) ranging from 0.70 to 0.75 (Table 3, Fig. 5). These fall in the range of BFI derived from monitoring data although the latter varies significantly among hydrograph separation methods, ranging from 0.5-0.63 by LMM, OPD, RDF, and ~0.9 by EMM. Despite the similar contribution of subsurface flow to total discharge, our simulations show that tile flow in RS and KS (~57%) has weaker impacts on discharge compared to LP and WW (~66%). The contribution of tile flow to discharge also differs among rainfall events. Tile flow accounts for a large proportion of peak flows in the ice-free season, especially for small and medium peaks. During heavy rainfalls, tile flow contributes to both rising and falling limbs, behaving as both quick and slow flows. (Fig. 5).

Similarly, the NO_3-N loads associated with subsurface flow are the dominant contributor to in-stream NO_3-N loads (Fig. 6 & Table S4). We found 77-81% of annual NO_3-N loads from these four catchments are carried by subsurface flows, in which tile flow is a dominant factor, delivering 53-76%. Lateral flow also plays an important role in delivering NO_3-N loads in RS (20%) and KS (23%) compared to LP (5%) and WW (6%). Surface runoff contributes to some peak loads during the winter season, but plays a marginal role in NO_3-N loads for small and median rainfall events. On the other hand, lateral flow dominates the NO_3-N loads during low flow periods.

3.3 Spatial Nitrate Leaching and Loading Dynamics

The model estimates reveal large spatial heterogeneity of NO_3-N leaching rates and accumulated NO_3-N loads along flow pathways, which vary among catchments (Fig. 7). Only a small proportion in the northeastern RS catchment has a high NO_3-N leaching rate (> 9 g N m^2 yr^{-1}), with the majority of the catchment showing a low level of NO_3-N leaching (< 5 g N m^2 yr^{-1}). Meanwhile, low NO_3-N loads along flow pathways are accumulated slowly within a large drainage area, especially in the central RS. In contrast, high NO_3-N leaching rates (> 7 g N m^2 yr^{-1}) are prevalent across the KS catchment compared with the other three catchments, contributing to high NO_3-N loads along the flow pathway delivered from a smaller drainage area. The northern end of the WW catchment exhibits a higher level of NO_3-N leaching rates (> 7 g N m^2 yr^{-1}) than that does its southern portion (< 5 g N m^2 yr^{-1}), resulting in a strong build-up of NO_3-N loads along the main catchment flow path. LP has an intermediate NO_3-N leaching rate from 5 to 9 g N m^2 yr^{-1} across the catchment. Furthermore, the discrepancy in NO_3-N leaching rates exists within the field. Grids with tile drainage and farmed potholes leach more NO_3-N from soils than non-tile drained, non-pothole grids.

3.4 Impacts of tile drainage and farmed potholes on water and NO_3-N fluxes

We examined the effects of tile drainage and farmed potholes in simulating flow-specific discharge and NO_3-N loading. Including tile drainage in the model substantially altered catchment-scale hydrological processes by reducing surface runoff (-25% − -45%) and lateral flow (-24% − -62%), while promoting tile flow (Fig. 8). By draining more water out of the soil, tile drainage also lowers evapotranspiration (-5% − -11%) while enhancing soil infiltration (7% − 19%) and increasing total discharge (11% − 50%). Adding farmed potholes into the model further enhances the tile flow (50% − 97%) with an increase in infiltration (16%) and reduction in surface runoff (-15% − -27%). Overall, the inclusion of tile drainage and farmed pothole jointly improved the accuracy of modeled stream discharge.

Similarly, simulated NO_3-N loading shows that including tile drainage in the model lowered the contribution of surface runoff (-41% − -49%) and lateral flow (-25% − -79%) to NO_3-N loads, with tile flow delivering the majority of NO_3-N loads (Fig. 9). In addition to the changes in different flows, including tile drainage increased total NO_3-N loads (18% − 94%). Conversely, adding farmed potholes slightly increased the NO_3-N export by tile flow (6% − 9%) and lateral flow (0.8% − 1%) while significantly reducing NO_3-N by surface runoff (-35% − -44%), resulting in lower total NO_3-N loads (-8% − -10%) compared with adding tile drainage alone. In general, the inclusion of tile drainage and farmed potholes improved model performance with respect to NO_3-N loading.

4 Discussion

4.1 Contribution of Different Flows to discharge and NO_3-N export

Quantifying the contribution of individual hydrological pathway to total water discharge is essential for accurately predicting the spatiotemporal dynamics of discharge and developing effective N reduction strategies in tile-drained agricultural watersheds in the U.S. Midwest. In this study, we compared the fraction of subsurface flow (tile flow and lateral flow) to total discharge using outputs from various hydrograph separation approaches and our model estimations (Table 3). The LMM, OPD, and RDF concluded a consistently low BFI in four catchments (50 to 63%). In contrast, the EMM and DLEM-catchment assessed a much higher BFI. Our model results are in agreement with other tile-drained watershed studies using a variety of base flow measures (Table 3). The LMM and two digital filter methods separate base flow and surface runoff with lines connecting low points of the stream hydrograph by assuming the rising limbs are caused by surface runoff. However, our daily simulation shows that tile flows also contribute to the rising and falling limbs of the hydrographs in these catchments, especially for peak flows of small and medium magnitudes (Fig. 5). This result has also been reported by several other researchers, using both empirical and modeling approaches (Ikenberry et al., 2017; Tomer et al., 2010). Therefore, these widely used hydrograph separation methods may underestimate the contribution of subsurface flows to stream discharge in the tile-drained watersheds.

Due to lower NO_3-N concentrations in surface runoff, our model simulated a higher proportion of annual subsurface flow to total NO_3-N loads (Table S4), with tile flow dominating both small and large peak loading during the growing season in each catchment (Fig. 5). Quantifying the flow-specific contribution of NO_3-N loading at the watershed scale is essential for implementing proper management practices (Arenas Amado et al., 2017). For example, riparian buffers have been reported to efficiently remove NO_3-N in surface runoff and shallow groundwater (Hill, 2019). However, our results suggest that the majority of NO_3-N loads might bypass stream buffers via tile drains, lowering their overall NO_3-N removal efficiency.

Furthermore, most studies focus on the separation of surface runoff and base flow but overlook the discrepancy among subsurface flows, such as interflow, tile drainage, and groundwater flows (Arenas Amado et al., 2017; Schilling et al., 2019). Our simulations show that despite the similar contributions from subsurface flows to total flows, the fractions of tile flow to discharge and NO_3-N loads are lower in RS and KS than those in LP and WW (Table 3). By measuring discharge and NO_3-N loads from all tile drain outlets and catchment outlets, Williams et al. (2015) estimated the contributions of tile flows to discharge (56-62%) that is consistent to our results for the RS and KS catchments. This is likely caused by the low tile-drained percentage in these two catchments, where a fair amount of water and NO_3-N is delivered by lateral flows from non-tile-drained grid cells. This indicates that the percent coverage of tile drainage influences the source compositions of discharge and NO_3-N load.

4.2 Spatial Variability of NO_3-N Leaching and Loading

The dynamics of stream NO_3-N loading are determined by local NO_3-N leaching and water transport networks within a catchment. By aggregating various environmental factors and landscape characteristics into a few sub-catchments or hydrologic units, semi-distributed water quality models tend to reduce the spatial variability of hydrological processes and aggregate flow transport networks. In contrast, the DLEM-catchment model features fully distributed flow networks embedded in grid cells with consideration of spatially explicit input data and coupled hydro-biogeochemical cycling, which makes it able to mimic complex N cycle processes and quantify the spatial heterogeneity of NO_3-N leaching in the study catchments (Fig. 7). Specifically, land characteristics, soil status, the presence of tile drains and farmed potholes govern the variability of NO_3-N leaching between and within each catchment. In addition, NO_3-N leaching rates also differ depending on cultivated crop types and N input levels (Kalkhoff et al., 2016). Our simulations show that grid cells that have high-level N input rates and tile drainage demonstrate the highest NO_3-N leaching rates. Interestingly, farmed potholes with tile installed underneath could intercept NO_3-N in surface runoff that route from the neighboring grid cells, forming hotspots of NO_3-N leaching in the areas with potholes. Meanwhile, DLEM-catchment is able to track the NO_3-N loading dynamics along flow pathways, which reflects the net changes between NO_3-N leaching, transport, and removal through the flow routing network over a given time period. For example, NO_3-N loads are slowly accumulated in central RS (< 1.5 Metric ton N yr^{-1}) due to general low NO_3-N leaching rates (< 5 g N m^{-2} yr^{-1}), whereas NO_3-N loads exceeding 1.5 Metric ton N yr^{-1} and NO_3-N leaching rates higher than 7 g N m^{-2} yr^{-1} from relatively smaller contributing areas are extensively found in KS. This implies that the prioritized catchments might be sought to cleaning water and reducing N footprint from agricultural landscape. Therefore, quantifying NO_3-N leaching and loading at a finer resolution (e.g. 30-m in this study) or at a scale where decision is made (e.g. field level) is essential for informing the spatial variations in NO_3-N pollution and identifying the critical areas to place the proper nitrogen reduction measures.

4.3 Key Model Developments Improving Model Performance

In this section, we examined how the key model development we made in this study, including modeling processes, structure, and inputs, has contributed to the improved model performance.

4.3.1 Water Retention Capacity and subsurface drainage

Snow processes: The two-layer snow module developed in this study mimics the snow properties, processes, and interactions with the soil surface, leading to better quantification of subsurface drainage and reproduces the continuous high-level of NO_3-N concentration as observed in winter in all the four catchments (Fig. 10a&11a). Seasonal snow plays a critical role in regulating catchment water balances during winter (Flanner et al., 2011). Snow accumulation not only collects snowfall and temporarily stores water in solid form, but also retains rainfall and meltwater within the snowpack porosity by refreezing capacity and capillary holding capacity, resulting in the reduction of surface runoff. Meanwhile, the insulating effect of the snowpack keeps soil from freezing and the gradual replenishment of water from melting snowpack into soil promotes infiltration and subsurface drainage (Ayers et al., 2021; Kalkhoff et al., 2016). Our results highlight the importance of accurately representing snow processes to improve simulation of winter hydrology and NO_3-N leaching in the watersheds with cold-season, especially in the tile-drained watersheds.

Soil Roughness: Our simulations show that adding soil roughness smooths small peaks during low flow and modestly reduces peak flows of higher magnitudes, indicating an enhancement in infiltration and subsurface flows (Fig. 10b). Additionally, our results indicate that considering soil roughness generally increases the model estimates of daily NO_3-N concentrations by enhancing the leaching of NO_3-N from soil with tile drainage (Fig. 11b). DLEM 2.0 estimates surface runoff as the combination of infiltration excess overland flow and saturation excess overland flow, based mainly on topographic characteristics and soil moisture states (Yang et al., 2015). This surface runoff generation mechanism has been employed in other grid-based spatially distributed hydrological models used in regional and global research (Niu et al., 2011). However, the soil roughness is enhanced by farming activities across cultivated fields in four agricultural catchments in this study, which significantly increases the importance of soil microrelief over topographic features in surface runoff generation. By increasing surface water storage, soil roughness impedes surface runoff and retains water in the agricultural watershed (Youssef et al., 2018).

Farmed Potholes: Farmed potholes perform important water regulating functions by impacting the magnitude, timing, and spatial patterns of flows in the prairie pothole region (Hayashi et al., 2016; Rajib et al., 2020). Most current hydrological models aggregate or lump potholes within HRUs to represent the combined hydrological functions of small depressions (Hay et al., 2018; Rajib et al., 2020). However, the conceptual lumping of potholes disconnects potholes among neighboring HRUs and overlooks fill-spill connections of potholes (Hayashi et al., 2016). Additionally, few studies have coupled N storage, retention, and transport to hydrological processes of potholes due to the lack of measurements and the complexity of modeling processes.

In this study, we linked the spatially explicit distribution of farmed potholes to the flow pathway network at 30-m resolution, allowing DLEM-catchment to simulate the water and N balance of individual potholes and their fill-spill connections. The simulated daily and annual discharge revealed that farmed potholes lowered peak flows while increasing subsurface flow (Fig. 10d), which is in agreement with previous modeling studies (Evenson et al., 2018). Interestingly, the simulated water level of farmed potholes demonstrates diverse roles of potholes in regulating hydrological balance depending on where they are located in their respective catchments (Fig. S5). For example, the potholes at the edge and upper reaches of the study catchments, where surface runoff contributing areas tend to be small, can fully intercept surface runoff from upstream grid cells (Fig. S5a-c). However, the potholes in the middle and lower reaches, where pothole contributing areas tend to be larger, mix and delay surface runoff through fill-spill process (Fig. S5d&e).

Our simulations show that depressions in the RS and KS catchments receive NO_3-N from surface runoff draining into the potholes, acting as local hotspots with elevated NO_3-N leaching (Fig. 7). This has been also observed in the in-field pothole research (Skopec and Evelsizer, 2018). Conversely, farmed potholes decrease the surface runoff NO_3-N loads while moderately increasing tile flow NO_3-N loads, performing as gatekeeper of catchment NO_3-N export (Fig. 9d & Fig. 11d). Our simulated NO_3-N removal effects by farmed potholes were consistent with field measurements and modeling estimates (Baron et al., 2013). The NO_3-N export reduction in the presence of potholes is likely caused by enhanced denitrification due to long NO_3-N residence time within these features (Golden et al., 2019). It is worth noting that the farmed potholes act as wetlands when filled with water, possessing water and nutrient regulating functions that we improved in this study. Therefore, these functions can be extended to catchments that include wetlands.

Tile drainage: It is well understood that artificial tile drains are the major contributor to discharge and nitrate loads in tile-drained watersheds (Arenas Amado et al., 2017; Helmers et al., 2005). Many modeling studies have adopted the physics-based Hooghoudt and Kirkham tile drain equations to estimate tile drainage (Ren et al., 2022; Singh et al., 2006). However, information about the parameters of the equations such as tile space, depth, and tube radius vary among fields and is often unavailable. Moreover, an accurate representation of surface depression depth, soil water movement, and water table dynamics is essential for tile drainage simulation. Our results show that the representation of tile drains in the DLEM-catchment has significantly improved estimations of discharge and NO_3-N export, in which catchment-specific parameters for describing the features of tile drains are important for reproducing daily observations. Specifically, tile drainage decreased peak flows, maintained high subsurface flow, and extended hydrograph recession (Fig. 10c), converting the subsurface flow to the dominant contributor to total discharge. However, removing tile drainage in the modeling scheme significantly enhanced in-stream NO_3-N concentrations during no-rain days because more NO_3-N will be accumulated in soils (Fig. 11c). More importantly, the interaction with water retention processes (e.g. soil roughness and farmed potholes) amplified the effects of tile drains. For example, the improved model with tile drainage and farmed potholes performed better than the model including tile drainage alone in predicting annual discharge and NO_3-N loading compared with observations (Fig. 8&9). Furthermore, the effects of tile drainage on water and NO_3-N in this study have broader applicability to other catchments characterized by artificial or natural subsurface drainage such as karst catchments.

4.3.2 Water and NO_3-N transport

Most fully distributed hydrological models assume that 1) surface runoff and subsurface flows generated in the grid are merged into the tributary or stream; and then 2) aggregated flows move to the downstream gird along the stream with the same transport speed. DLEM-catchment, however, routes surface runoff and subsurface flows separately (with distinct different travel times) to the downstream grid because the delivery-scale catchments are small in size and only contains water and nutrient movement before they reach streams. In addition, tile drains transport water far more quickly than untiled subsurface drainage (Schilling et al., 2015), and as such it is necessary to consider its water and nutrient transport processes in a way different from other flows. Therefore, in this study we developed a new flow routing network in the model structure with separated flow pathways and individual travel times to capture the dominant flow transport pathways and processes in tile-drained agricultural landscapes (Fig. 2). This new conceptual structure also enables the DLEM-catchment to link farmed potholes to surface runoff routing. In this model, flow travel time was calculated based on grid-level factors such as slope, soil properties, and management, reflecting the variability of catchment characteristics. As a result, due to the large difference in NO_3-N concentration among flows, the improvement in flow routing can benefit the estimation of NO_3-N transport and delivery.

4.3.3 Agricultural Management

Agricultural management such as crop rotation, tillage, cover crops, and synthetic and manure N fertilizer use (including application rate, timing, method, and fertilizer type) have direct and indirect impacts on the water and NO_3-N balances of farmed watersheds (Kaspar et al., 2012). However, due to the difficulty in obtaining explicit management information at the scale of individual fields, modeling research often uses static data from the literature, regional averages, or management guidance provided by university extension offices (Ikenberry et al., 2017; Ren et al., 2022). Neglecting the spatiotemporal heterogeneity of agricultural management has fed models with biased inputs and generated large uncertainties in estimating the magnitude and timing of discharge and NO_3-N export. DLEM 2.0 has evolved to use various agricultural management information for regional assessments (Lu et al., 2022, 2020; Yu et al., 2018). Additionally, in this study, we prescribed the time-series field-level management information to each catchment at a resolution of 30 m and modified relevant model processes to address the spatiotemporal representation of these management practices. We found the modeling estimates have well reproduced observed inter-annual and seasonal variations of NO_3-N exports for four study catchments, capturing the rise of observed NO_3-N concentration in early spring and late fall, and corresponding declines in summer. This success could be largely attributed to the improved input information including crop planting date and N fertilizer application timings at the field level. Additionally, fine-scale management data we used in this study enables the model to reflect the divergent magnitude of in-stream NO_3-N concentrations across catchments, and spatial heterogeneity of NO_3-N leaching and loading. The adequate representation of anthropogenic management in our model, and the reasonable accuracy of the model with respect to discharge and outlet NO_3-N concentrations shows that DLEM-catchment has the potential to be a capable decision support tool.

4.4 Uncertainties and Limitations

Model performance is largely affected by the quality of input data, including the accuracy of precipitation time-series, assumed spatial distributions of tile drains, and agricultural management information. The precipitation data was extracted from spatially interpolated precipitation maps. Therefore, the rainfall amount is averaged and may be smaller than that from individual sites within the region, especially with respect to local storms. Moreover, due to the limited climate data availability, we used daily precipitation data as water inputs, which may underestimate rainfall intensity and generation of surface runoff during brief storms. These factors may explain why DLEM-catchment underestimates some large peak flows and corresponding NO_3-N concentration dilution in our simulations (Fig. 3&4).

Due to the lack of detailed information about the hydraulic characteristics of tile drains and their locations, the tile drained grids are determined based on gSSURGO soil drainage classes. Given the impacts of tile drains on flows and N exports, this limitation may be significant. Despite having field-level agricultural management information from partnering farmers, the management records for about half of the fields within each catchment remain unavailable and are assumed to be identical to other known fields with close cropping system in a given year. The lack of spatially explicit management information in these fields may also introduce uncertainties in the simulated results.

Some simplified model processes and structure may also limit the model performance. For example, we developed a new model structure to represent flow pathways and individual flow travel time, by which different flows are constrained within the corresponding flow path from grid to grid with no intersections. However, in reality, interflow that flows above the tile drains may enter tiles in downstream grids. On the other hand, when soils of downstream girds are unsaturated, surface runoff from upstream grids may enter the soil through infiltration, which could increase the proportion of subsurface flow to total discharge. The simplification we made to exclude flow interactions may explain the lower BFI estimated by our model compared to the EMM approach. We also simplified the biogeochemical processes in farmed potholes, such as crop mortality and enhanced denitrification caused by inundation (Hayashi et al., 2016; LaBaugh et al., 2018). As potholes cover a small portion of drainage areas in the study catchments, this likely have little impacts on simulated water discharge and NO_3-N loading, but more measurement data within potholes will improve model capability in quantifying potential hot spot contributions. It is worth noting that the delivery-scale catchments have short-distance perennial streams, in which in-stream N biogeochemical cycling has little impacts on NO_3-N loading. DLEM-catchment may need further improvements in stream N biogeochemical processes for predicting NO_3-N loading in large-scale watersheds.

5 Conclusions

In this study, using the spatially distributed process-based DLEM-catchment model, we identified and quantified the key model processes and features that are critical for accurately simulating water discharge and NO_3-N exports from four tile-drained catchments in the Midwestern US. We also comprehensively quantified the flow-specific contributions to and cross-catchment variations in water flow and NO_3-N fluxes under various weather and management conditions. The improved model reasonably reproduced the dynamics of discharge and NO_3-N fluxes, with satisfactory performance for daily simulations and good performance for monthly simulations. Particularly, tile drains coupled with water retention capacity from snow processes, soil roughness, and farmed potholes substantially alter the water and NO_3-N balances of these catchments by promoting infiltration and subsurface drainage, while decreasing surface runoff. Agricultural management practices, such as crop planting/harvesting, and fertilizer input rates and timing, play an essential role in regulating NO_3-N leaching at a daily time step. These model performance improvements verify the necessity of considering these mechanisms in tile-drained watersheds in the US rain-fed Corn Belt areas. Meanwhile, the water balance and NO_3-N dynamic regulating functions by these improvements can be transferred to other models designed for different types of catchments.

The improved model estimated reasonable ranges of event-based and annual flow-specific contributions to discharge and NO_3-N loading compared with other hydrograph separation approaches and other studies in the tile-drained catchments. Daily simulations show that tile flow is the dominant contributor to peak flows, especially for small and medium peaks, while lateral flow dominates low flows during dry periods. At the annual scale, the model estimates that subsurface flow (tile flow and lateral flow) accounts for 70%-75% of discharge and 77%-82% of NO_3-N loading. However, tile flow contributes more water and NO_3-N loads in the LP and WW catchments than the other two catchments due to a larger proportion of poorly-drained areas with no tile drains, indicating the necessity to quantify tile flow and lateral flow separately. Our simulated results reveal that the contributions of different flows to discharge and NO_3-N loading vary significantly among catchments and among rainfall events depending on local conditions.

With the adequate representation of various agricultural management and coupled hydrological-biogeochemical-processes, the improved model results demonstrate the detailed spatial patterns of hydrological NO_3-N losses within catchments. Agricultural management (e.g. N fertilizer and manure application rate and timing), which varies across fields, notably impacts the magnitude and seasonality of NO_3-N leaching. Landscape characteristics (e.g. geographic slope and farmed potholes), soil properties, and artificial tile drainage govern local NO_3-N loss dynamics. Our study highlighted the importance of integrating cross-scale water quality monitoring catchment characteristics, and in-field management practices into a water quality modeling framework for improving prediction accuracy and identifying effective N reduction strategies. In general, our findings illustrate the necessity of modeling tools like DLEM-catchment to assess and predict the effectiveness of management practices in reducing NO_3-N loading from tile-drained agricultural landscapes.

Acknowledgement

We acknowledge funding support from National Science Foundation (#1945036, #1903722), and Iowa Nutrient Research Center (#2017-06, #2018-13, #2021-05). We also appreciate two anonymous reviewers for their construction comments in improving this manuscript.

Reference

Arenas Amado, A., Schilling, K.E., Jones, C.S., Thomas, N., Weber, L.J., 2017. Estimation of tile drainage contribution to streamflow and nutrient loads at the watershed scale based on continuously monitored data. Environ. Monit. Assess. 189, 426. https://doi.org/10.1007/s10661-017-6139-4

Ayers, J.R., Villarini, G., Schilling, K., Jones, C., 2021. On the statistical attribution of changes in monthly baseflow across the U.S. Midwest. J. Hydrol. 592, 125551. https://doi.org/https://doi.org/10.1016/j.jhydrol.2020.125551

Baron, J.S., Hall, E.K., Nolan, B.T., Finlay, J.C., Bernhardt, E.S., Harrison, J.A., Chan, F., Boyer, E.W., 2013. The interactive effects of excess reactive nitrogen and climate change on aquatic ecosystems and water resources of the United States. Biogeochemistry 114, 71–92. https://doi.org/10.1007/s10533-012-9788-y

Bian, Z., Tian, H., Yang, Q., Xu, R., Pan, S., Zhang, B., 2021. Production and application of manure nitrogen and phosphorus in the United States since 1860. Earth Syst. Sci. Data 13, 515–527. https://doi.org/10.5194/essd-13-515-2021

Cao, P., Lu, C., Yu, Z., 2018. Historical nitrogen fertilizer use in agricultural ecosystems of the contiguous United States during 1850–2015: application rate, timing, and fertilizer types. Earth Syst. Sci. Data 10, 969–984. https://doi.org/10.5194/essd-10-969-2018

Crumpton, W.G., Stenback, G.A., Fisher, S.W., Stenback, J.Z., Green, D.I.S., 2020. Water quality performance of wetlands receiving nonpoint-source nitrogen loads: Nitrate and total nitrogen removal efficiency and controlling factors. J. Environ. Qual. 49, 735–744. https://doi.org/https://doi.org/10.1002/jeq2.20061

Du, B., G. Arnold, J., Saleh, A., B. Jaynes, D., 2005. Development and application of SWAT to landscapes with tiles and potholes. Trans. ASAE 48, 1121–1133. https://doi.org/https://doi.org/10.13031/2013.18522

Eckhardt, K., 2005. How to construct recursive digital filters for baseflow separation. Hydrol. Process. 19, 507–515. https://doi.org/https://doi.org/10.1002/hyp.5675

Evenson, G.R., Golden, H.E., Lane, C.R., McLaughlin, D.L., D'Amico, E., 2018. Depressional wetlands affect watershed hydrological, biogeochemical, and ecological functions. Ecol. Appl. 28, 953–966. https://doi.org/https://doi.org/10.1002/eap.1701

Flanner, M.G., Shell, K.M., Barlage, M., Perovich, D.K., Tschudi, M.A., 2011. Radiative forcing and albedo feedback from the Northern Hemisphere cryosphere between 1979 and 2008. Nat. Geosci. 4, 151–155. https://doi.org/10.1038/ngeo1062

Golden, H.E., Rajib, A., Lane, C.R., Christensen, J.R., Wu, Q., Mengistu, S., 2019. Non-floodplain Wetlands Affect Watershed Nutrient Dynamics: A Critical Review. Environ. Sci. Technol. 53, 7203–7214. https://doi.org/10.1021/acs.est.8b07270

Gonzalo, R., Pablo, M.J., A., T.F., Réka, H., G., C.K., Patricio, G., 2022. Climate and agronomy, not genetics, underpin recent maize yield gains in favorable environments. Proc. Natl. Acad. Sci. 119, e2113629119. https://doi.org/10.1073/pnas.2113629119

Gupta, H. V, Kling, H., Yilmaz, K.K., Martinez, G.F., 2009. Decomposition of the mean squared error and NSE performance criteria: Implications for improving hydrological modelling. J. Hydrol. 377, 80–91. https://doi.org/https://doi.org/10.1016/j.jhydrol.2009.08.003

Hay, L., Norton, P., Viger, R., Markstrom, S., Steven Regan, R., Vanderhoof, M., 2018. Modelling surface-water depression storage in a Prairie Pothole Region. Hydrol. Process. 32, 462–479. https://doi.org/https://doi.org/10.1002/hyp.11416

Hayashi, M., van der Kamp, G., Rosenberry, D.O., 2016. Hydrology of Prairie Wetlands: Understanding the Integrated Surface-Water and Groundwater Processes. Wetlands 36, 237–254. https://doi.org/10.1007/s13157-016-0797-9

Helmers, M.J., Lawlor, P., Baker, J.L., Melvin, S., Lemke, D., 2005. Temporal subsurface flow patterns from fifteen years in north-central iowa. 2005 ASAE Annu. Int. Meet.

Hill, A.R., 2019. Groundwater nitrate removal in riparian buffer zones: a review of research progress in the past 20 years. Biogeochemistry 143, 347–369. https://doi.org/10.1007/s10533-019-00566-5

Hill, R.A., Fox, E.W., Leibowitz, S.G., Olsen, A.R., Thornbrugh, D.J., Weber, M.H., 2017. Predictive mapping of the biotic condition of conterminous U.S. rivers and streams. Ecol. Appl. 27, 2397–2415. https://doi.org/https://doi.org/10.1002/eap.1617

IEM (Iowa Environmental Mesonet), 2021. National Weather Service Cooperative 787 Observer Program [WWW Document]. URL https://mesonet.agron.iastate.edu/request/coop/fe.phtml?network=IACLIMATE

Ikenberry, C.D., Soupir, M.L., Helmers, M.J., Crumpton, W.G., Arnold, J.G., Gassman, P.W., 2017. Simulation of Daily Flow Pathways, Tile-Drain Nitrate Concentrations, and Soil-Nitrogen Dynamics Using SWAT. JAWRA J. Am. Water Resour. Assoc. 53, 1251–1266. https://doi.org/https://doi.org/10.1111/1752-1688.12569

Jones, C.S., Nielsen, J.K., Schilling, K.E., Weber, L.J., 2018. Iowa stream nitrate and the Gulf of Mexico. PLoS One 13, e0195930.

Kalkhoff, S.J., Hubbard, L.E., Tomer, M.D., James, D.E., 2016. Effect of variable annual precipitation and nutrient input on nitrogen and phosphorus transport from two Midwestern agricultural watersheds. Sci. Total Environ. 559, 53–62. https://doi.org/https://doi.org/10.1016/j.scitotenv.2016.03.127

Kaspar, T.C., Jaynes, D.B., Parkin, T.B., Moorman, T.B., Singer, J.W., 2012. Effectiveness of oat and rye cover crops in reducing nitrate losses in drainage water. Agric. Water Manag. 110, 25–33. https://doi.org/10.1016/j.agwat.2012.03.010

LaBaugh, J.W., Rosenberry, D.O., Mushet, D.M., Neff, B.P., Nelson, R.D., Euliss, N.H., 2018. Long-term changes in pond permanence, size, and salinity in Prairie Pothole Region wetlands: The role of groundwater-pond interaction. J. Hydrol. Reg. Stud. 17, 1–23. https://doi.org/10.1016/j.ejrh.2018.03.003

Liu, M., Tian, H., Yang, Q., Yang, J., Song, X., Lohrenz, S.E., Cai, W.-J., 2013. Long-term trends in evapotranspiration and runoff over the drainage basins of the Gulf of Mexico during 1901–2008. Water Resour. Res. 49, 1988–2012.

https://doi.org/https://doi.org/10.1002/wrcr.20180

Lu, C., Yu, Z., Hennessy, D.A., Feng, H., Tian, H., Hui, D., 2022. Emerging weed resistance increases tillage intensity and greenhouse gas emissions in the US corn–soybean cropping system. Nat. Food 3, 266–274. https://doi.org/10.1038/s43016-022-00488-w

Lu, C., Zhang, J., Cao, P., Hatfield, J.L., 2019. Are We Getting Better in Using Nitrogen?: Variations in Nitrogen Use Efficiency of Two Cereal Crops Across the United States. Earth's Futur. 7, 939–952. https://doi.org/10.1029/2019EF001155

Lu, C., Zhang, J., Tian, H., Crumpton, W.G., Helmers, M.J., Cai, W.-J., Hopkinson, C.S., Lohrenz, S.E., 2020. Increased extreme precipitation challenges nitrogen load management to the Gulf of Mexico. Commun. Earth Environ. 1. https://doi.org/10.1038/s43247-020-00020-7

Lyne, V., Hollick, M., 1979. Stochastic time-variable rainfall-runoff modelling, in: Institute of Engineers Australia National Conference. Institute of Engineers Australia Barton, Australia, pp. 89–93.

McDeid, S.M., Green, D.I.S., Crumpton, W.G., 2019. Morphology of Drained Upland Depressions on the Des Moines Lobe of Iowa. Wetlands 39, 587–600. https://doi.org/10.1007/s13157-018-1108-4

Moriasi, D.N., Gitau, M.W., Pai, N., Daggupati, P., 2015. Hydrologic and Water Quality Models: Performance Measures and Evaluation Criteria. Trans. ASABE 58, 1763–1785. https://doi.org/https://doi.org/10.13031/trans.58.10715

Nash, J.E., Sutcliffe, J. V, 1970. River flow forecasting through conceptual models part I — A discussion of principles. J. Hydrol. 10, 282–290. https://doi.org/https://doi.org/10.1016/0022-1694(70)90255-6

Niu, G.Y., Yang, Z.L., Mitchell, K.E., Chen, F., Ek, M.B., Barlage, M., Kumar, A., Manning, K., Niyogi, D., Rosero, E., Tewari, M., Xia, Y., 2011. The community Noah land surface model with multiparameterization options (Noah-MP): 1. Model description and evaluation with local-scale measurements. J. Geophys. Res. Atmos. 116, 1–19. https://doi.org/10.1029/2010JD015139

Rajib, A., Golden, H.E., Lane, C.R., Wu, Q., 2020. Surface Depression and Wetland Water Storage Improves Major River Basin Hydrologic Predictions. Water Resour. Res. 56, 1–19. https://doi.org/10.1029/2019WR026561

Ren, D., Engel, B., Mercado, J.A.V., Guo, T., Liu, Y., Huang, G., 2022. Modeling and assessing water and nutrient balances in a tile-drained agricultural watershed in the U.S. Corn Belt. Water Res. 210, 117976. https://doi.org/https://doi.org/10.1016/j.watres.2021.117976

Schilling, K.E., Gassman, P.W., Arenas-Amado, A., Jones, C.S., Arnold, J., 2019. Quantifying the contribution of tile drainage to basin-scale water yield using analytical and numerical models. Sci. Total Environ. 657, 297–309. https://doi.org/https://doi.org/10.1016/j.scitotenv.2018.11.340

Schilling, K.E., Helmers, M., 2008. Effects of subsurface drainage tiles on streamflow in Iowa agricultural watersheds: Exploratory hydrograph analysis. Hydrol. Process. 22, 4497–4506.

https://doi.org/https://doi.org/10.1002/hyp.7052

Schilling, K.E., Jones, C.S., 2019. Hydrograph separation of subsurface tile discharge. Environ. Monit. Assess. 191. https://doi.org/10.1007/s10661-019-7377-4

Schilling, K.E., Wolter, C.F., Isenhart, T.M., Schultz, R.C., 2015. Tile Drainage Density Reduces Groundwater Travel Times and Compromises Riparian Buffer Effectiveness. J. Environ. Qual. 44, 1754–1763. https://doi.org/10.2134/jeq2015.02.0105

Singh, R., Helmers, M.J., Qi, Z., 2006. Calibration and validation of DRAINMOD to design subsurface drainage systems for Iowa's tile landscapes. Agric. Water Manag. 85, 221–232. https://doi.org/10.1016/j.agwat.2006.05.013

Skopec, M., Evelsizer, V., 2018. Spring Nutrient Levels in Drained Wetlands of IOWA's Prairie Pothole Region. Wetlands 38, 261–273. https://doi.org/10.1007/s13157-017-0962-9

Sloto, R.A., Crouse, M.Y., 1996. HYSEP: A computer program for streamflow hydrograph separation and analysis. Water-resources Investig. Rep. 96, 4040.

Tahmasebi Nasab, M., Chu, X., 2020. Macro-HyProS: A new macro-scale hydrologic processes simulator for depression-dominated cold climate regions. J. Hydrol. 580, 124366. https://doi.org/https://doi.org/10.1016/j.jhydrol.2019.124366

Tian, H., Chen, G., Liu, M., Zhang, C., Sun, G., Lu, C., Xu, X., Ren, W., Pan, S., Chappelka, A., 2010. Model estimates of net primary productivity, evapotranspiration, and water use efficiency in the terrestrial ecosystems of the southern United States during 1895–2007. For. Ecol. Manage. 259, 1311–1327. https://doi.org/https://doi.org/10.1016/j.foreco.2009.10.009

Tomer, M.D., Meek, D.W., Jaynes, D.B., Hatfield, J.L., 2003. Evaluation of Nitrate Nitrogen Fluxes from a Tile-Drained Watershed in Central Iowa. J. Environ. Qual. 32, 642–653. https://doi.org/https://doi.org/10.2134/jeq2003.6420

Tomer, M.D., Wilson, C.G., Moorman, T.B., Cole, K.J., Heer, D., Isenhart, T.M., 2010. Source-pathway separation of multiple contaminants during a rainfall-runoff event in an artificially drained agricultural watershed. J. Environ. Qual. 39, 882–895. https://doi.org/10.2134/jeq2009.0289

Valayamkunnath, P., Barlage, M., Chen, F., Gochis, D.J., Franz, K.J., 2020. Mapping of 30-meter resolution tile-drained croplands using a geospatial modeling approach. Sci. Data 7, 257. https://doi.org/10.1038/s41597-020-00596-x

Wei, Y., Liu, S., Huntzinger, D.N., Michalak, A.M., Viovy, N., Post, W.M., Schwalm, C.R., Schaefer, K., Jacobson, A.R., Lu, C., Tian, H., Ricciuto, D.M., Cook, R.B., Mao, J., Shi, X., 2014. The North American Carbon Program Multi-scale Synthesis and Terrestrial Model Intercomparison Project – Part 2: Environmental driver data. Geosci. Model Dev. 7, 2875–2893. https://doi.org/10.5194/gmd-7-2875-2014

Wellen, C., Kamran-Disfani, A.-R., Arhonditsis, G.B., 2015. Evaluation of the Current State of Distributed Watershed Nutrient Water Quality Modeling. Environ. Sci. Technol. 49, 3278–3290. https://doi.org/10.1021/es5049557

Williams, M.R., King, K.W., Fausey, N.R., 2015. Contribution of tile drains to basin discharge and nitrogen export in a headwater agricultural watershed. Agric. Water Manag. 158, 42–50. https://doi.org/https://doi.org/10.1016/j.agwat.2015.04.009

Yang, Q., Tian, H., Friedrichs, M.A.M., Hopkinson, C.S., Lu, C., Najjar, R.G., 2015. Increased nitrogen export from eastern North America to the Atlantic Ocean due to climatic and anthropogenic changes during 1901–2008. J. Geophys. Res. Biogeosciences 120, 1046–1068. https://doi.org/https://doi.org/10.1002/2014JG002763

Youssef, M.A., Abdelbaki, A.M., Negm, L.M., Skaggs, R.W., Thorp, K.R., Jaynes, D.B., 2018. DRAINMOD-simulated performance of controlled drainage across the U.S. Midwest. Agric. Water Manag. 197, 54–66. https://doi.org/https://doi.org/10.1016/j.agwat.2017.11.012

Yu, Z., Lu, C., Cao, P., Tian, H., 2018. Long-term terrestrial carbon dynamics in the Midwestern United States during 1850–2015: Roles of land use and cover change and agricultural management. Glob. Chang. Biol. 24, 2673–2690. https://doi.org/10.1111/gcb.14074

Zhang, J., Cao, P., Lu, C., 2021. Half-Century History of Crop Nitrogen Budget in the Conterminous United States: Variations Over Time, Space and Crop Types. Global Biogeochem. Cycles 35, e2020GB006876. https://doi.org/https://doi.org/10.1029/2020GB006876

Zhang, J., Lu, C., Crumpton, W., Jones, C., Tian, H., Villarini, G., Schilling, K., Green, D., 2022. Heavy Precipitation Impacts on Nitrogen Loading to the Gulf of Mexico in the 21st Century: Model Projections Under Future Climate Scenarios. Earth's Futur. 10, e2021EF002141. https://doi.org/https://doi.org/10.1029/2021EF002141

Table 1. Characteristics of the four catchments.

Characteristics		Unit	RS	KS	LP	WW
Landscape	Drainage area	km^2	4.6	3.0	2.1	2.4
	Mean Slope	%	0.86	0.93	0.43	0.77
	Farmed Potholes	%	7.5	3.3	0	0
Climate*	Annual Tem	°C	9.2	10.3	8.3	8.3
	PPT	mm	1019	1066	1183	1176
Row crop	Fields[#]		19	18	9	15
	CS	%	27	37	56	31
	CCS	%	24	17	7	21
	CCC	%	40	36	27	26
Management	Total N input	g N m^{-2} yr^{-1}	10.3-22.5	14.1-20.5	18.6-23.8	9.9-20.2
	N fer / Manure	%	6-100	0-100	100	0-100
	Fall application	%	0-94	0-100	0-32	18-100
	Cover Crop	%	47	0	85	0
	Tile coverage	%	55	62	89	88

*Climate conditions shown here are the annual average values during 2015-2019. Annual Tem is annual mean temperature. PPT is annual total precipitation. Number of fields is counted by the boundary of fields defined by partnering farmers and CDL (cropland Data Layer) maps. The cropping systems are defined by time-series crop type and rotation categories according to the 30-m CDL data: CS is corn-soybean rotation, CCS is corn-corn-soybean rotation, and CCC is three and more consecutive corn years. Cover crop was implemented in fall 2017. Total N input includes N fertilizer and manure N.

Table 2. Statistic indices of model performance in estimating discharge, and NO_3-N concentration and loads at the daily and monthly scale.

Watershed	Variables	Daily			Monthly		
		NSE	PBIAS	KGE	NSE	PBIAS	KGE
RS	Q	0.62*	-5.7**	0.79**	0.73**	-5.7**	0.85**
	NO_3-N conc.	0.34	0.2***	0.64*	0.46*	-0.1***	0.69*
	NO_3-N load	0.54**	-4.0***	0.77**	0.70***	-3.9***	0.85**
KS	Q	0.64*	14.0*	0.69*	0.80***	13.9*	0.84**
	NO_3-N conc.	0.35*	-3.4***	0.55*	0.50**	-2.1***	0.60**
	NO_3-N load	0.15	12.4**	0.56*	0.68***	13.9**	0.77**
LP	Q	0.58*	-14.1*	0.75**	0.86***	-14.4**	0.83**
	NO_3-N conc.	0.15	-10.0***	0.61*	0.39*	-10.4***	0.71*
	NO_3-N load	0.52**	-26.9*	0.63*	0.68***	-27*	0.66*
WW	Q	0.57*	-6.4***	0.77**	0.82***	-6.6***	0.89**
	NO_3-N conc.	0.42*	-8.9***	0.64*	0.68***	-5.0***	0.63*
	NO_3-N load	0.50**	-20.0**	0.58*	0.71***	-18.8***	0.74*

* represents satisfactory, ** is good, *** is very good only for NSE and PBIAS (Criteria can be found in *Supplementary Table S3*).

Table 3. Comparison between this study and other studies in quantifying the contribution from tile drainage and subsurface flow to annual discharge.

Watershed	Drainage Area (km^2)	Tile Drain (%)	Subsurface Flow (%)	Tool*	Citations
LCW-LCR4T	2.5		62	RDF	Schilling and Jones (2019)
LCW-LCR3T	6.0		61	RDF	
KS	3.1		75	EMMM	Ikenberry et al. (2017)
			73	SWAT	
AL	2.3		89	EMMM	
			85	SWAT	
UBWC-B	3.9	56 62		Measurement	Williams et al. (2015)
LCW	42	66	~76	SWAT	Schilling et al. (2019)
WCW	51		75	DRAINMOD	Schilling and Helmers (2008)
RS	4.6		60	RDF	This study
			63	OPD	
			53	LMM	
			91	EMM	
		59	72	DLEM	
KS	3.0		54	RDF	
			55	OPD	
			54	LMM	
			87	EMM	
		56	71	DLEM	
LP	2.1		56	RDF	
			58	OPD	
			60	LMM	
			90	EMM	
		70	75	DLEM	
WW	2.4		50	RDF	
			50	OPD	
			53	LMM	
			90	EMM	
		62	70	DLEM	

*RDF is Recursive Digital Filter, EMM is End-Member-Mix-Model, SWAT is Soil Water Assessment Tool. OPD is One Parameter Digital filter. LMM represents Local Minimum Method.

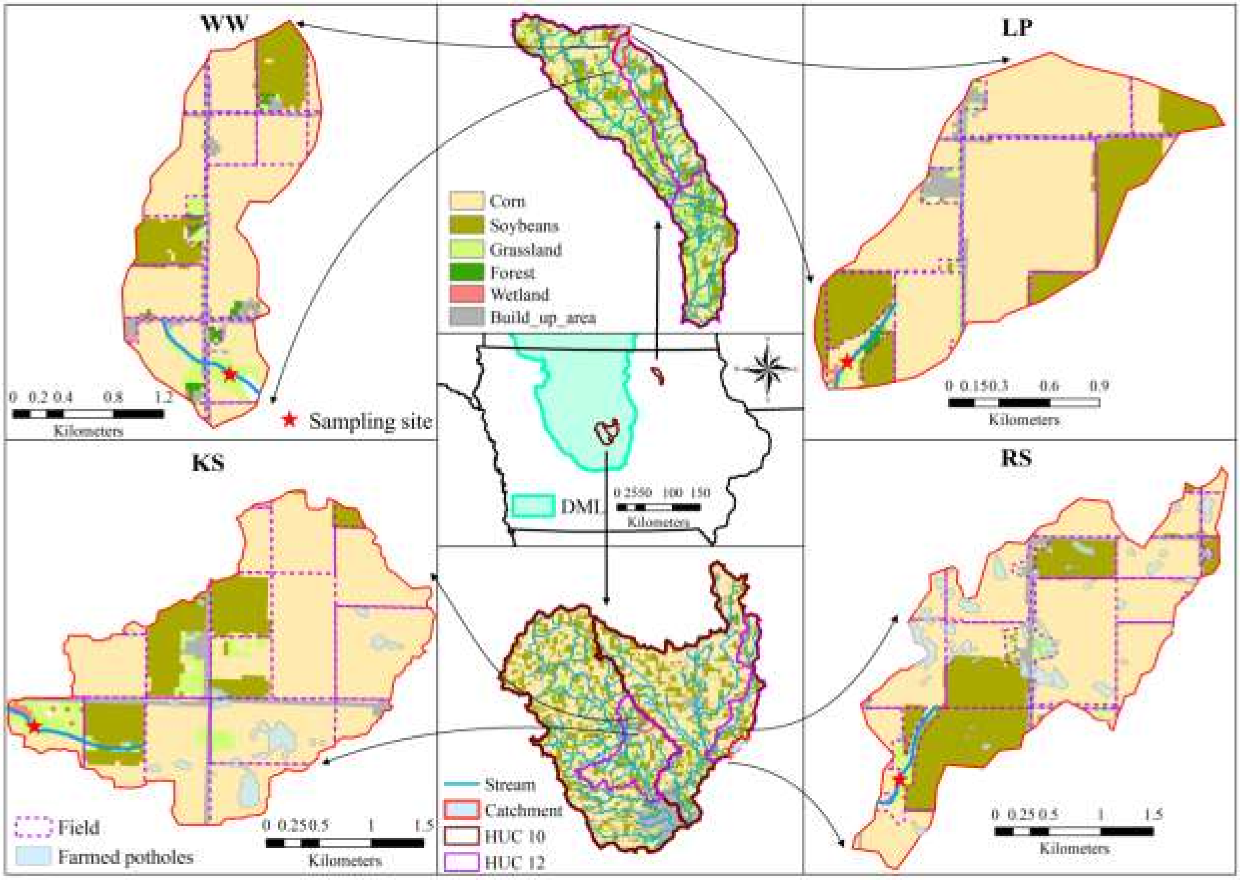

Figure 1. Land use map of the four study catchments in Iowa (i.e., RS, KS, LP, and WW) with sampling locations shown by the star symbol (we use the land use maps in 2016 as an example). DML refers to Des Moines Lobe. HUC 10 refers to Hydrologic Unit Code 10 with an average spatial scale of 590 km^2. HUC 12 refers to Hydrologic Unit Code 12 with an average spatial scale of 100 km^2.

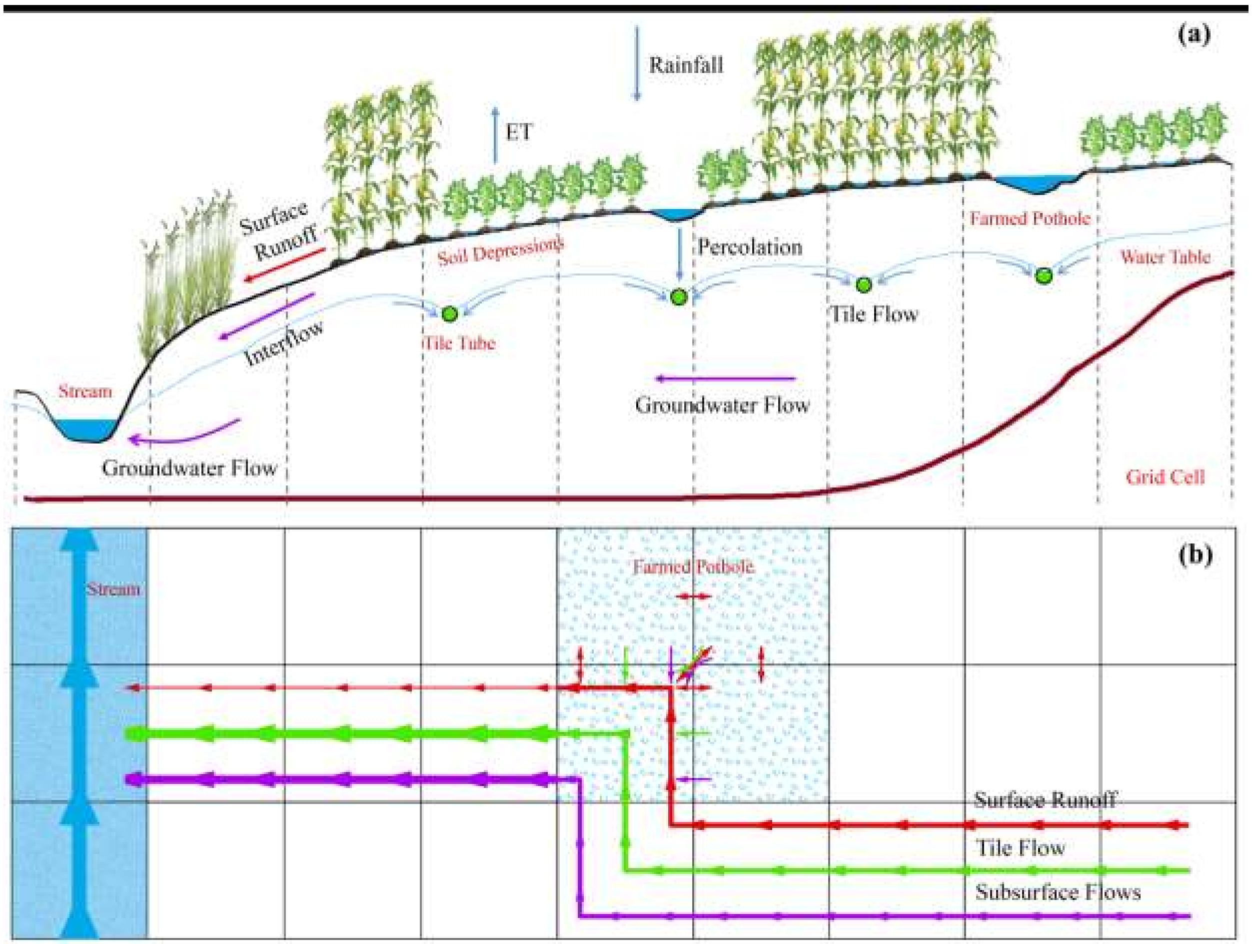

Figure 2. (a) Conceptual framework to show the hydrological processes that is represented in model for tile-drained catchments, and (b) Grid-based flow pathway and the interactions between flows and farmed potholes. Subsurface Flows refer to Interflow and Groundwater Flow in (a), of which the travel time is unequal.

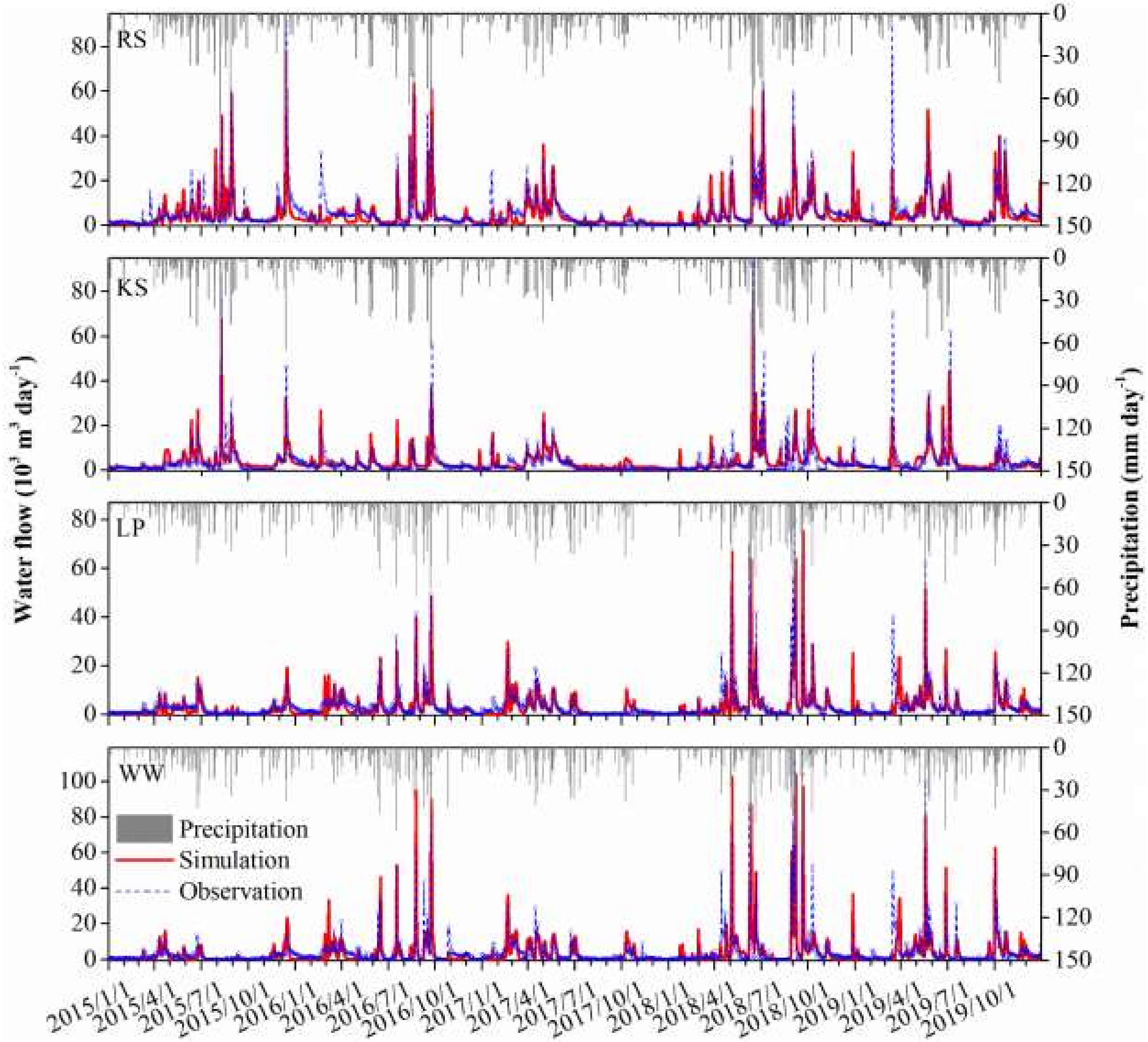

Figure 3. Comparison of model-estimated vs. monitored daily water discharge amount at four tile-drained catchments in Central Iowa during 2015-2019.

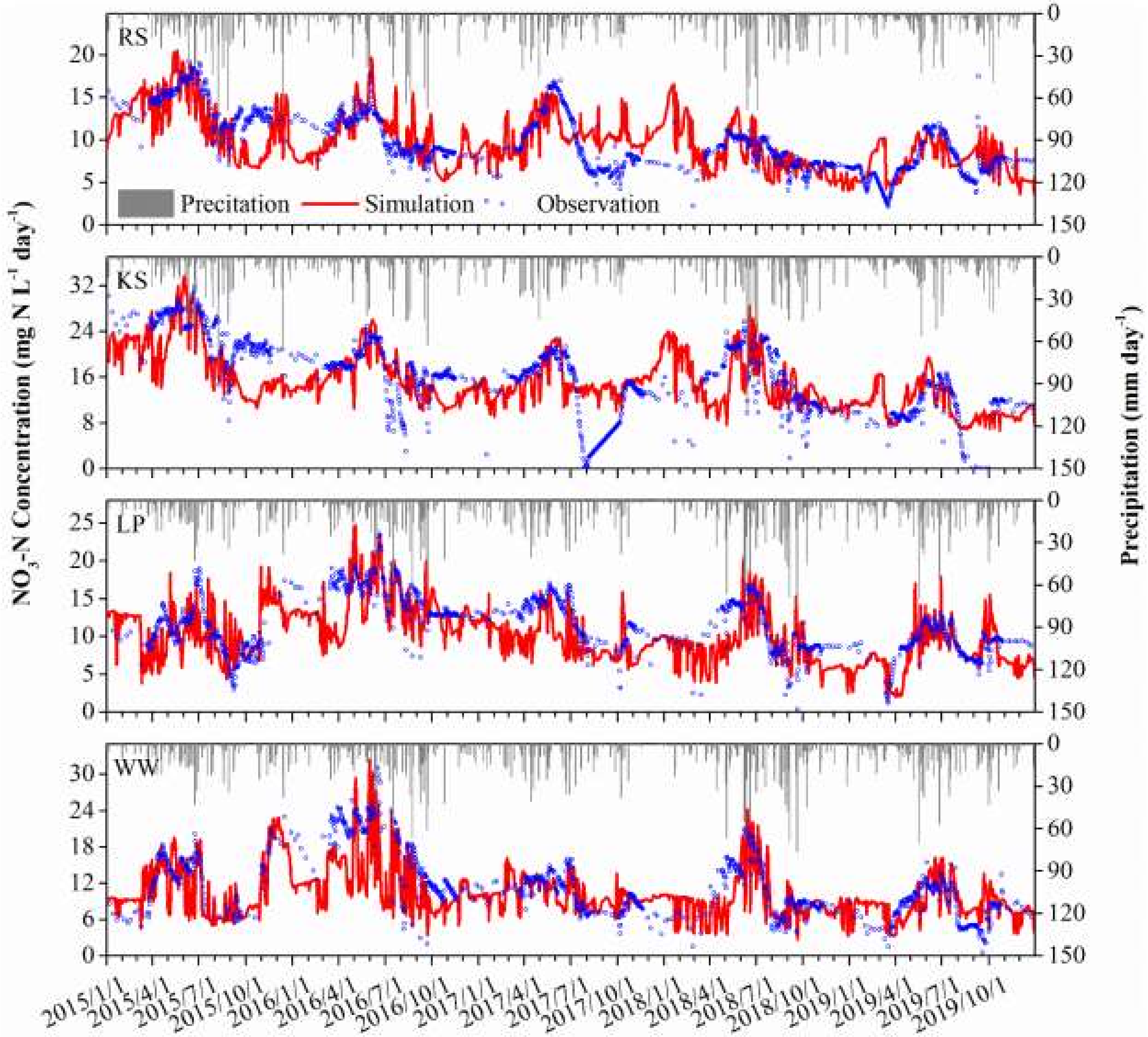

Figure 4. Comparison of daily NO_3-N concentration between simulation and observation at the four catchments during 2015-2019.

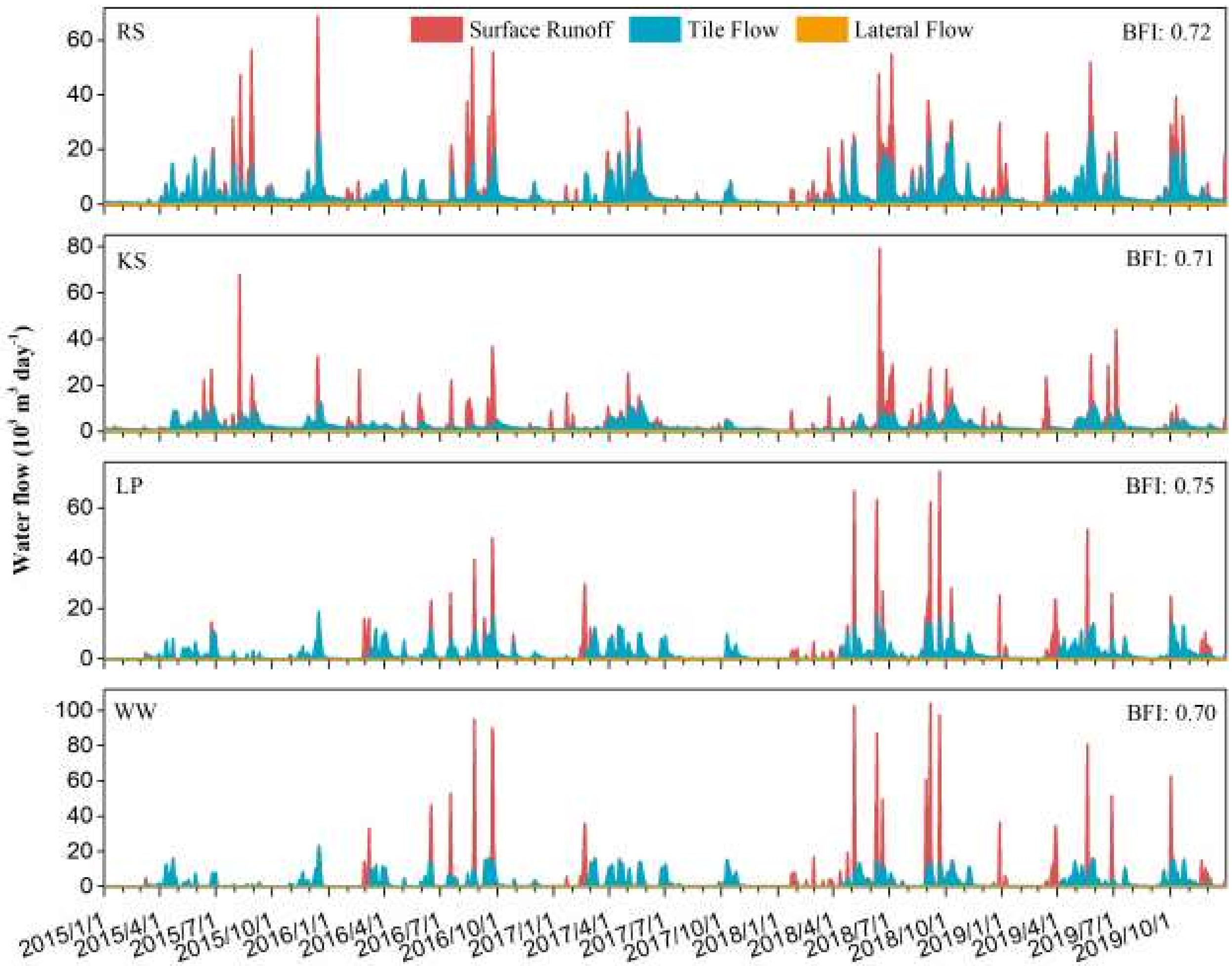

Figure 5. Simulated daily surface runoff, tile flow, and lateral flow at the outlet of four catchments. Lateral flow includes interflow and groundwater flow. BFI is the 5-y-average ratio of subsurface flow (tile flow + lateral flow) to discharge from 2015 to 2019.

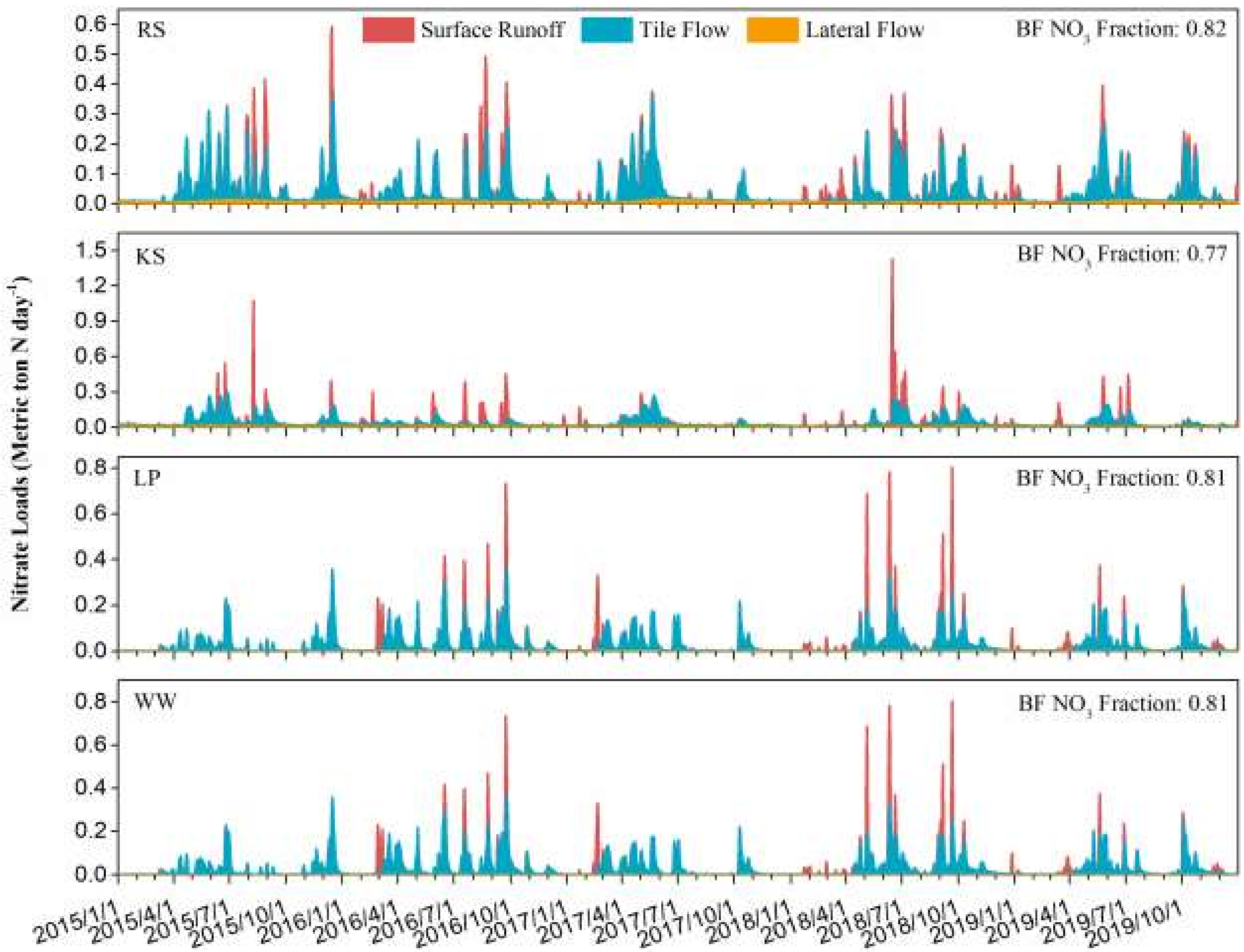

Figure 6. Simulated daily NO_3-N loads of surface runoff, tile flow, and lateral flow at the outlet of four catchments. Lateral flow includes interflow and groundwater flow. BF NO_3-N fraction is the 5-yr average fraction of NO_3-N loads carried by subsurface flow (tile flow + lateral flow) in the total NO_3-N loads from 2015 to 2019.

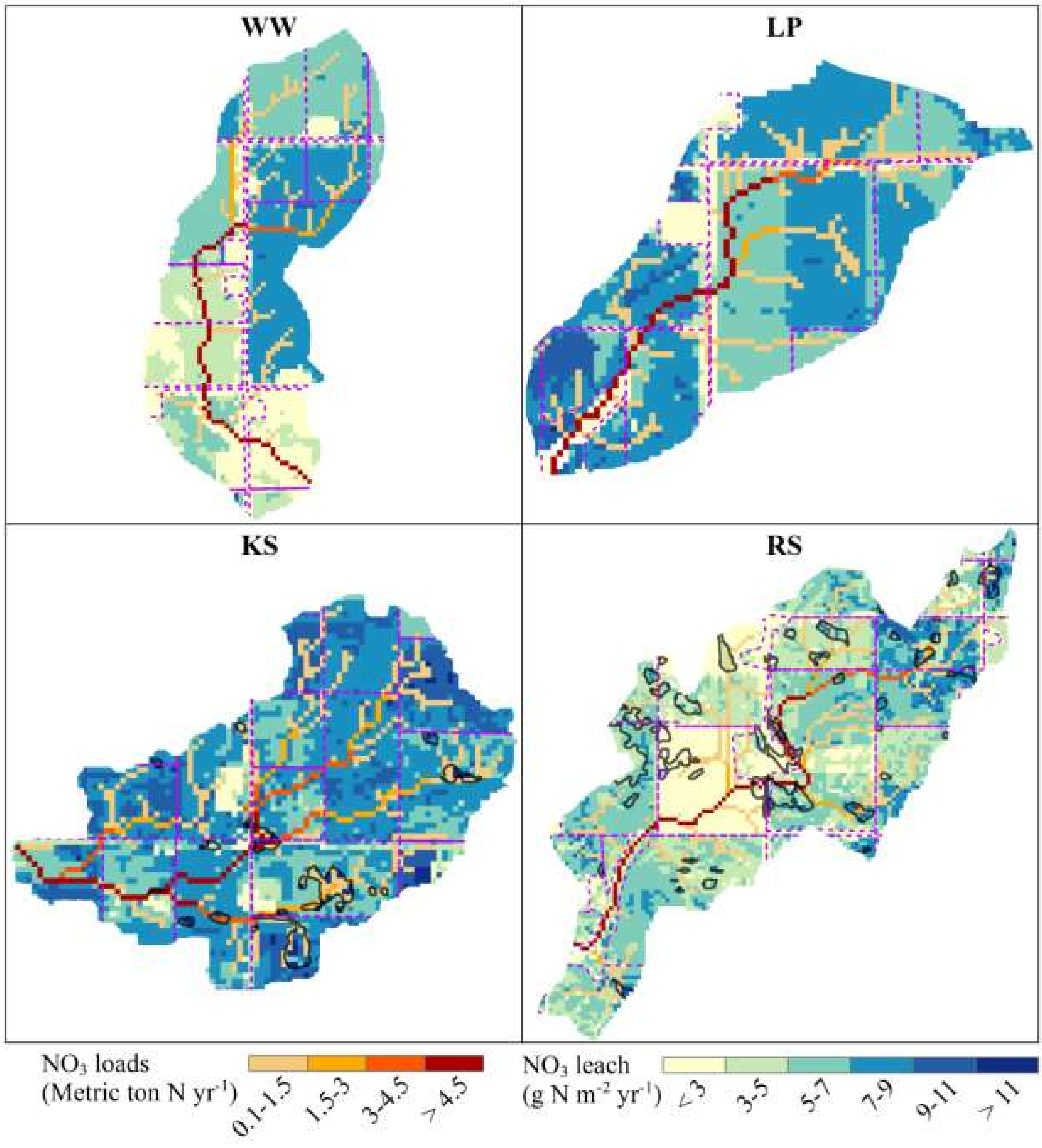

Figure 7. Spatial distribution of model-estimated annual average NO_3-N leaching and loading in four catchments over 2015-2019 with a resolution of 30 m ×30 m.

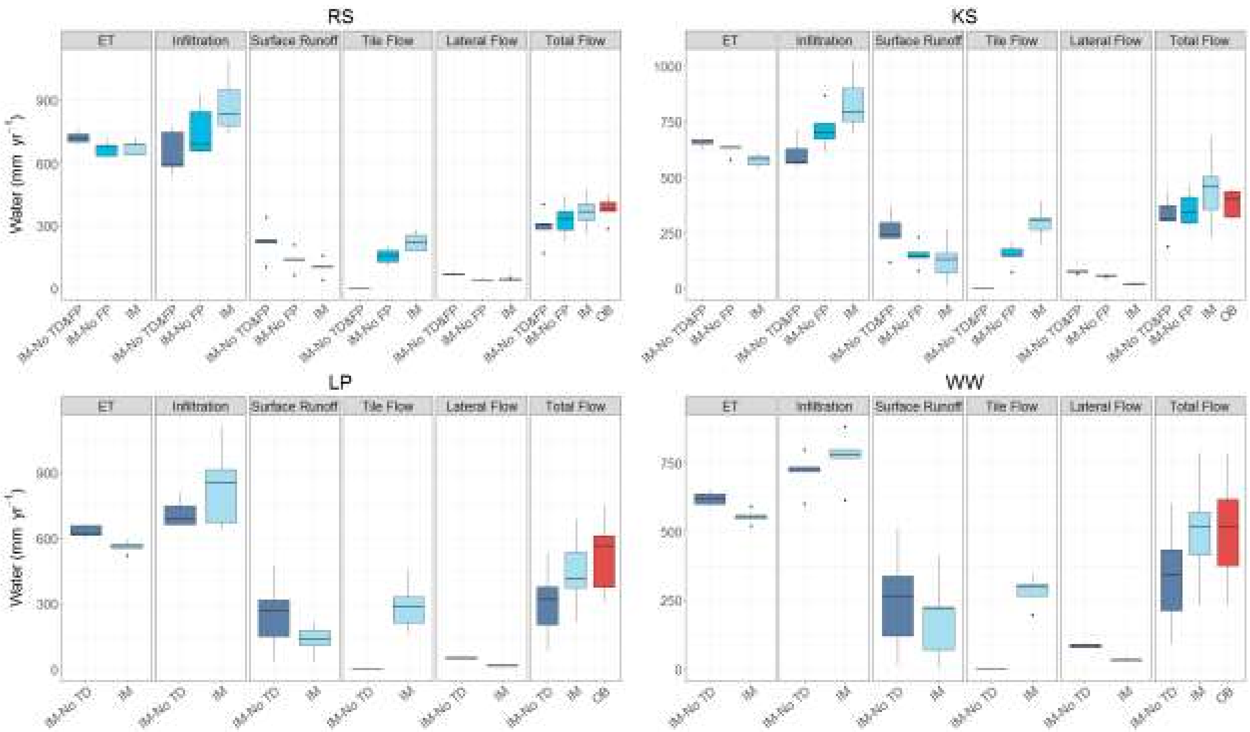

Figure 8. The model-estimated water balance components, including ET, infiltration, surface runoff, tile flow, lateral flow, and total flow, were derived from multiple model structures and comparison with total flow observations (OB, red bar) during 2015-2019. Lateral flow aggregates interflow and groundwater flow. IM represents the Improved Model. IM-No TD represents the improved model without Tile Drainage. IM-No TD & FP represents the improved model without Tile Drainage and Farmed Pothole. The upper and lower hinge of the box indicate 25-75% quantile, respectively. Black lines are medium values, and whiskers comprise the whole range of data.

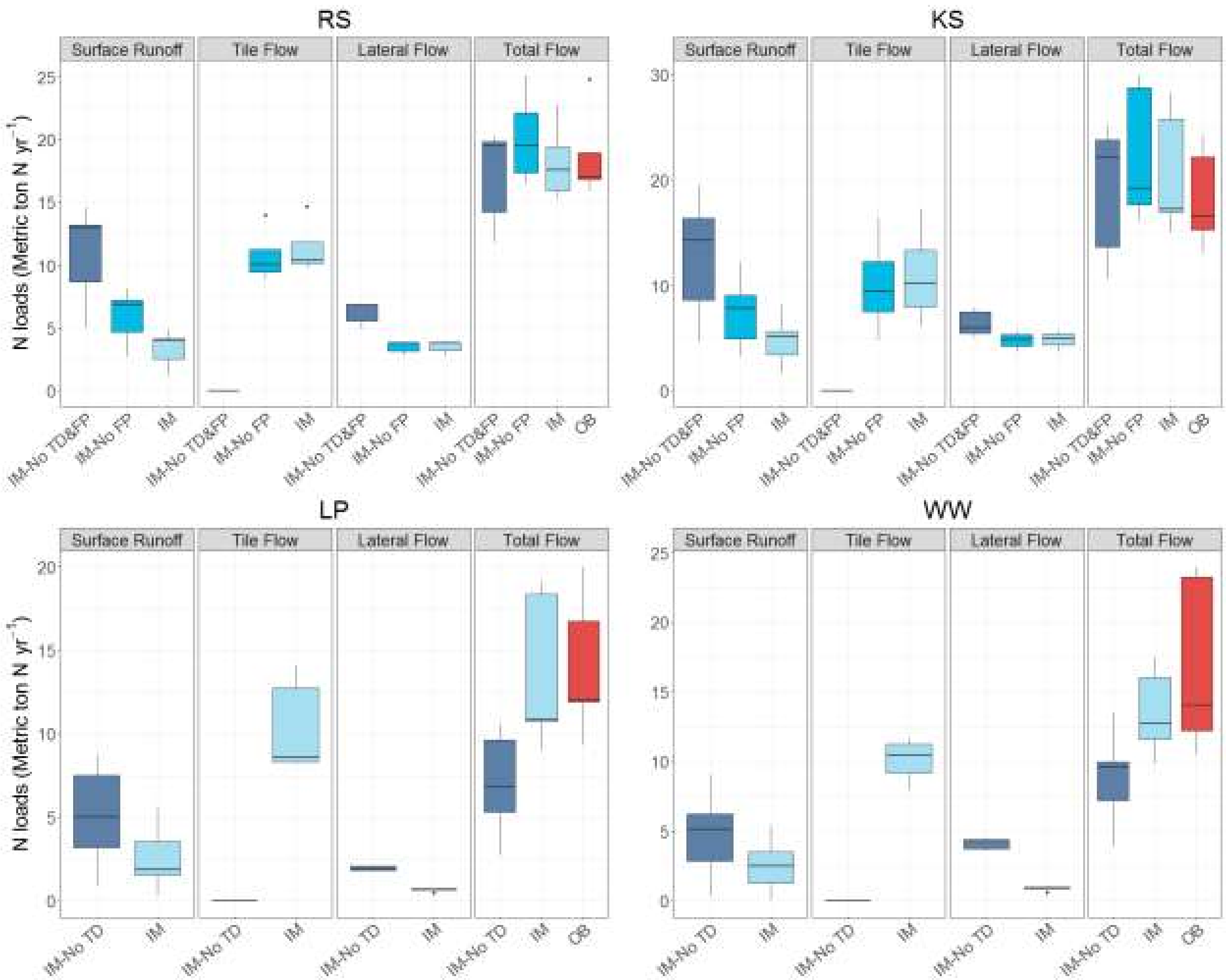

Figure 9. NO_3-N delivered by different water flows as estimated by multiple model structures and compared with total NO_3-N load observations (OB, red bar). Lateral flow aggregates NO_3-N loads from interflow and groundwater flow. IM represents Improved Model. TD represents Tile Drainage. FP represents Farmed Pothole. Boxes include 25-75% of NO_3-N loading during 2015-2019, black lines are medium values, and whiskers comprise the whole range of data.

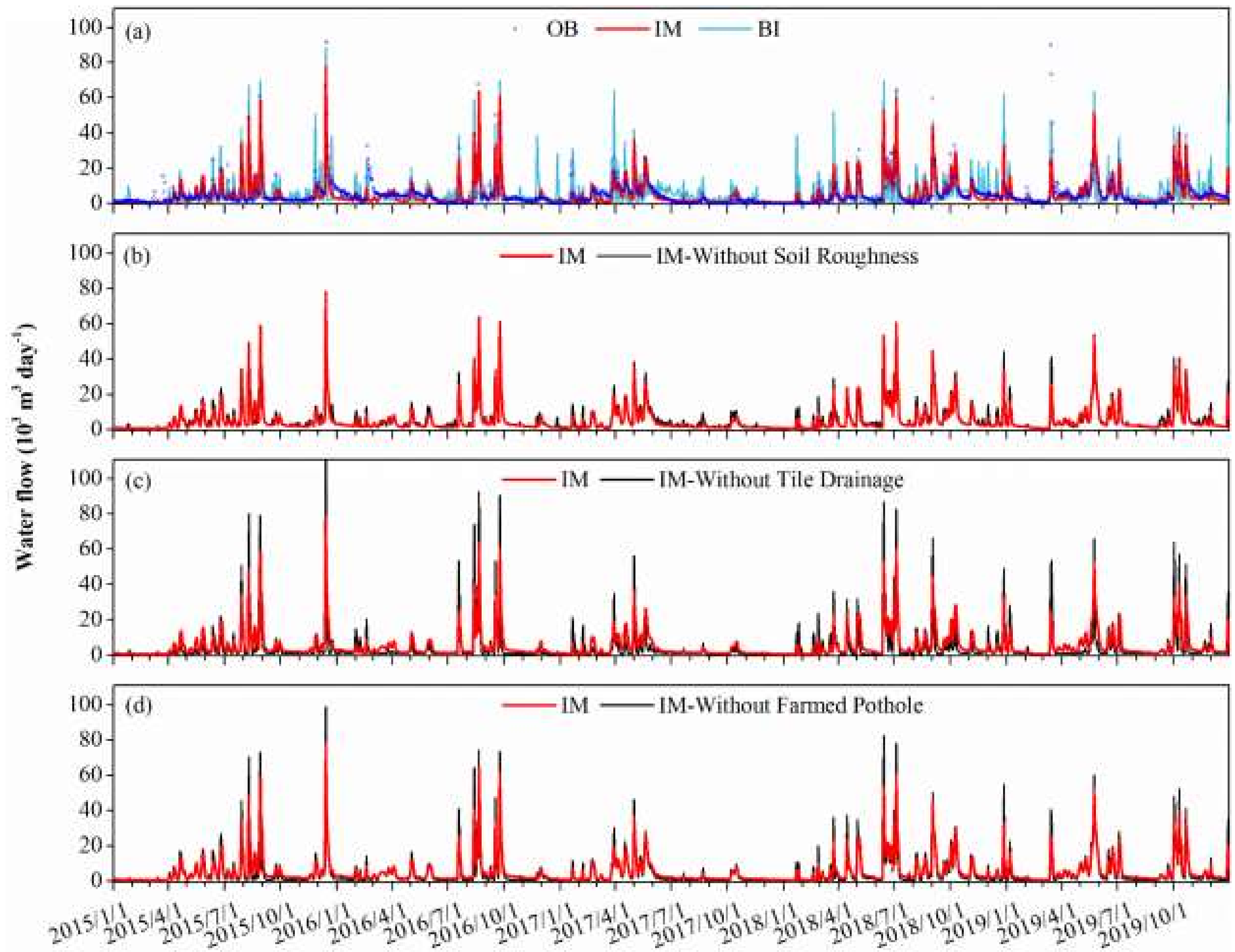

Figure 10. Improved model performance in simulating daily water discharge (a) and contributions of key model structure reflected by comparing estimations between improved model (IM) and IM without a certain feature (b-d). OB represents observation, BI represents model estimates before Improvement. IM represents Improved Model estimates.

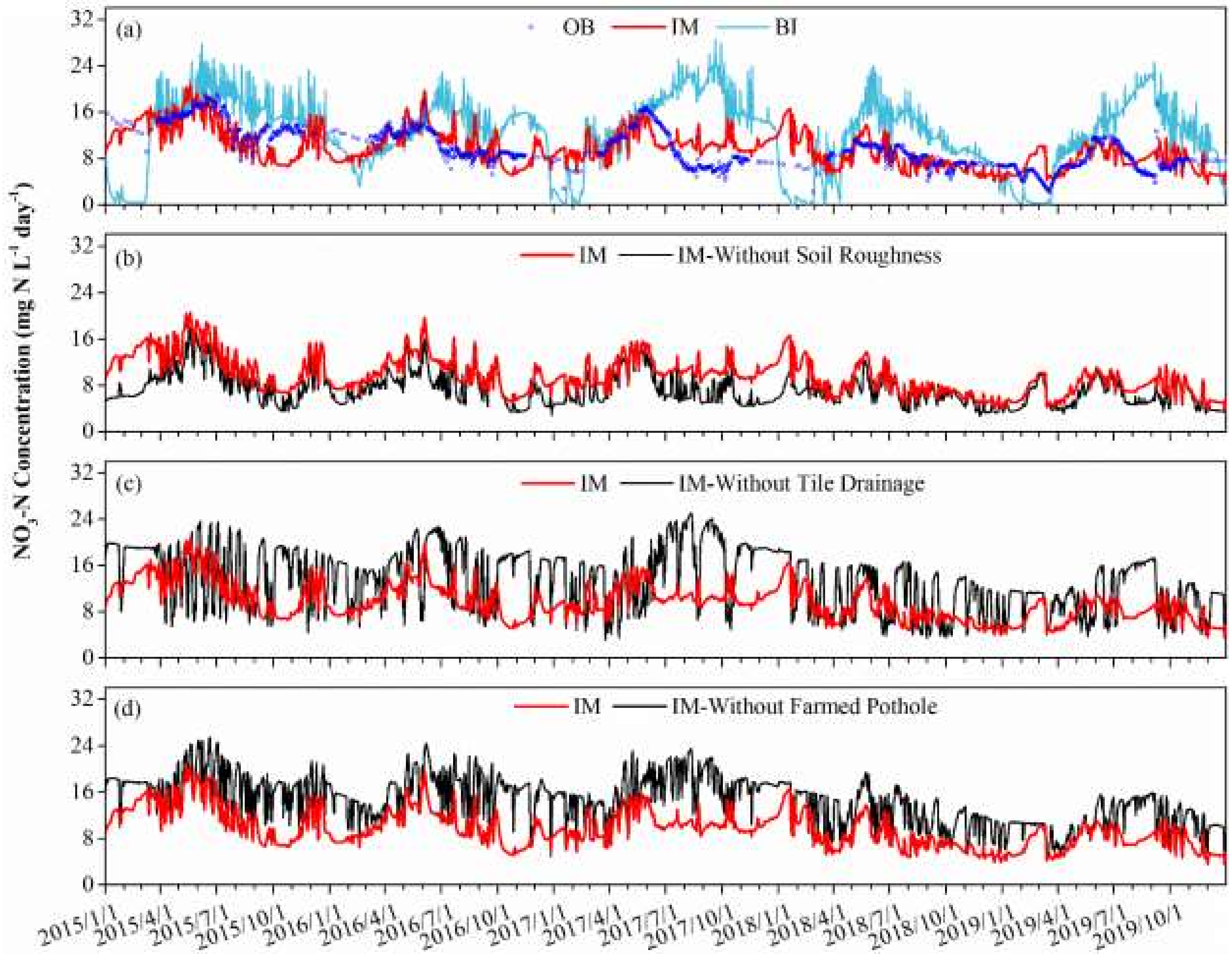

Figure 11. Improved model performance in simulating daily NO_3-N concentration (a) and contributions of key model structure reflected by comparing estimations between improved model (IM) and IM without a certain feature (b-d). OB represents Observation. BI represents model estimates before Improvement.